Sensors and Actuators A 214 (2014) 58–65

Contents lists available at ScienceDirect

Sensors and Actuators A: Physical

journal homepage: www.elsevier.com/locate/sna

Deterministic and band-limited stochastic energy harvesting from uniaxial excitation of a multilayer piezoelectric stack

S. Zhao, A. Erturk*

G. W. Woodruff School of Mechanical Engineering, Georgia Institute of Technology, Atlanta, GA 30332, USA

ARTICLE INFO

Article history:
Received 24 November 2013
Received in revised form 10 April 2014
Accepted 11 April 2014
Available online 23 April 2014

Keywords:
Energy harvesting
Piezoelectricity
Deterministic
Stochastic
Stack

ABSTRACT

Deterministic and band-limited stochastic energy harvesting scenarios using a multilayer piezoelectric stack configuration are investigated for uniaxial dynamic pressure loading. The motivation for exploring this off-resonant energy harvesting problem derives from typical civil infrastructure systems subjected to dynamic compressive forces in deterministic or stochastic forms due to vehicular or human loads, among other examples of compressive loading. Modeling of vibrational energy harvesters in the existing literature has been mostly focused on deterministic forms of mechanical vibration as in the typical case of harmonic excitation, while the efforts on stochastic energy harvesting have thus far considered second-order systems such as piezoelectric cantilevers. In this paper, we present electromechanical modeling, analytical and numerical solutions, and experimental validations of piezoelectric energy harvesting from harmonic, periodic, and band-limited stochastic excitation of a multilayer piezoelectric stack under axial compressive loading in the off-resonant low-frequency range. The deterministic problem employs the voltage output-to-pressure input frequency response function of the harvester for a given electrical load, which is also extended to periodic excitation. The analytical stochastic electromechanical solution employs the power spectral density of band-limited stochastic excitation to predict the expected value of the power output. The first one of the two numerical solution methods uses the Fourier series representation of the excitation history to solve the resulting ordinary differential equation, while the second method employs an Euler–Maruyama scheme to directly solve the governing electromechanical stochastic differential equation. The electromechanical models are validated through several experiments for a multilayer PZT-5H stack under harmonic and band-limited stochastic excitations at different pressure levels. The figure of merit is also extracted for this particular energy harvesting problem to choose the optimal material. Soft piezoelectric ceramics (e.g. PZT-5H and PZT-5A) offer larger power output as compared to hard ceramics (e.g. PZT-8), and likewise, soft single crystals (e.g. PMN-PT and PMN-PZT) produce larger power as compared to their hard counterparts (e.g. PMN-PZT-Mn); and furthermore, single crystals (e.g. PMN-PT and PMN-PZT) generate more power than standard ceramics (e.g. PZT-5H and PZT-5A) for low-frequency, off-resonant excitation of piezoelectric stacks.

1. Introduction

Vibration-based energy harvesting for low-power electricity generation has received growing attention over the last decade [1–4]. The motivation in this research field is due to the reduced power requirement of small electronic components, such as wireless sensor networks used in passive and active monitoring applications. By means of harvesting ambient energy in next-generation wireless electronic systems, it is aimed to minimize the maintenance costs for periodic battery replacement/charging as well as the chemical waste of conventional batteries. Over the last decade, numerous research groups have reported their work on modeling and applications of vibration/kinetic energy harvesting using electromagnetic [5–10], electrostatic [11–13], piezoelectric [14–20], magnetostrictive [21,22], and electrostrictive [23,24] conversion mechanisms, as well as electronic and ionic electroactive polymers [25,26]. In particular, due to the high power density and ease of application of piezoelectric materials in various configurations from meso-scale [15,17] to micro-scale [27–30], piezoelectric energy harvesting has received the greatest attention [3,31–34].

The existing literature of piezoelectric energy harvesting has mostly explored cantilevers whereas very limited work has focused

* Corresponding author. Tel.: +1 404 385 1394; fax: +1 404 894 8496.
E-mail address: alper.erturk@me.gatech.edu (A. Erturk).

http://dx.doi.org/10.1016/j.sna.2014.04.019
0924-4247/

on piezoelectric stacks [35–37]. Goldfarb and Jones [38] analyzed a piezoelectric stack under harmonic mechanical load using a lumped parameter model and derived an expression of power efficiency. Feenstra et al. [39] designed an energy harvester that employed a mechanically amplified piezoelectric stack and converted the dynamic tension in the backpack strap to electrical energy. As an alternative to conventional flex-tensional piezoelectric transducer [40], Li et al. [41] designed a flex-compressive mode transducer that used two piezoelectric stacks and two bow-shaped elastic plates for energy harvesting.

In terms of stochastic (random) vibrational energy harvesting, the entire literature of energy harvesting has focused on second-order (resonating) linear and nonlinear configurations. Stochastic vibration energy harvesting models for standard second-order linear energy harvesters under broadband excitation were given by Halvorsen [42] and Adhikari et al. [43]. Stochastic analysis using distributed-parameter piezoelectric energy harvester models including higher vibration modes was presented by Zhao and Erturk [44]. In addition to stochastic energy harvesting with linear stiffness [42–44], researchers have also explored stochastic excitation of second-order monostable [45,46] and bistable [47–53] nonlinear energy harvesters of Duffing oscillator type. However, stochastic excitation of first-order energy harvesters (such as a piezoelectric stack configuration excited within typical ambient energy frequency spectrum) by dynamic pressure loading has not been addressed to date. Typically the fundamental resonance frequency of a stack-type piezoelectric energy harvester under uniaxial loading (one the order of tens of kHz) is much higher than arguably all practical ambient excitation frequency spectra, resulting in first-order dynamic behavior.

The present work investigates deterministic and stochastic energy harvesting scenarios using a multilayer piezoelectric stack under dynamic pressure loading. The motivation for exploring this off-resonant energy harvesting problem derives from typical civil infrastructure systems subjected to dynamic compressive forces in deterministic or band-limited stochastic forms due to vehicular or human loads, among other examples of compressive loading in low-frequency region of piezoelectric stacks. In the following, first, an electromechanical model is given along with frequency response derivations for the modeling of harmonic and periodic excitation cases. The figure of merit to choose the optimal piezoelectric material is also extracted. After that, both analytical and numerical solutions of power generation from band-limited stochastic excitation are summarized. Finally, experimental results are presented to validate the analytical and numerical predictions of low-power electricity generation from harmonic and stochastic uniaxial loading.

2. Deterministic excitation and electromechanical response

2.1. Governing electromechanical equation

Fig. 1 shows a multilayer piezoelectric stack energy harvester configuration under the excitation of dynamic pressure $p(t)$ in the axial direction (3-direction). The formulation given in the following assumes that the highest frequency content of the axial pressure is much lower than the fundamental resonance frequency of the stack so that one-way coupling and first-order behavior can describe the electromechanical system dynamics.[1] If the total of N thickness-poled layers in the stack are connected in parallel to a resistive

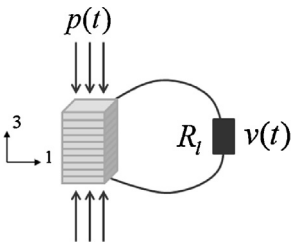

Fig. 1. Schematic of a multilayer piezoelectric stack used for harvesting energy from uniaxial dynamic pressure excitation at off-resonant low frequencies (thickness-poled piezoelectric layers are combined in parallel).

electrical load (R_l), then the governing circuit equation is obtained from

$$\sum_{i=1}^{N} \frac{d}{dt}\left(\int_{A_i} \mathbf{D}\cdot\mathbf{n}dA_i\right) = \frac{v(t)}{R_l}, \tag{1}$$

where $v(t)$ is the voltage response across the load, $\mathbf{D}$ is the vector of electric displacements, $\mathbf{n}$ is the vector of surface normal of the electrodes, and the integration of their inner product is performed over the electrode area A_i of the ith layer. The electric displacement components are obtained from

$$D_i = d_{ijk}T_{jk} + \varepsilon_{ij}^{T}E_j, \tag{2}$$

where T_{jk} and E_j are the stress and electric field tensors, respectively, d_{ijk} is the tensor of piezoelectric strain constants, and ε_{ij}^{T} is the tensor of permittivity constants at constant stress. If contracted index notation (i.e. Voigt's notation: $11\rightarrow1, 22\rightarrow2, 33\rightarrow3, 23\rightarrow4, 13\rightarrow5, 12\rightarrow6$) is used in Eq. (1) along with the electrode and mechanical boundary conditions, the surviving stress ($T_3 = p(t)$) and electric field ($E_3 = -v/h$, where h is the thickness of each piezoelectric layer) components yield the governing electromechanical equation

$$C_p^{eq}\dot{v}(t) + \frac{1}{R_l}v(t) = d_{33}^{eff}A\dot{p}(t), \tag{3}$$

where C_p^{eq} is the equivalent capacitance and d_{33}^{eff} is the effective piezoelectric constant, A is the cross-sectional area on which the pressure is acting (thus $p(t)A$ is the dynamic force transmitted to the stack), and an over-dot represents differentiation with respect to time. For a stack made of N identical layers, the effective piezoelectric strain constant and equivalent capacitance are $d_{33}^{eff} = N\mu d_{33}$ and $C_p^{eq} = N\lambda\varepsilon_{33}^{T}A/h$, where μ and λ are empirical constants that account for the difference between the bulk and thin-layer piezoelectric and dielectric constants as well as the fabrication effects on the stack (μ and λ are close to unity). The dielectric loss of is assumed to be negligible (although it can be taken into account by assuming a complex permittivity constant). Once again, the highest frequency content ($\bar{\omega}$) of the dynamic pressure is assumed to be much lower than the fundamental natural frequency of the stack (ω_n), i.e. $\bar{\omega} \ll \omega_n$; therefore the stress field is insensitive to changing electrical load resistance, making it possible to represent the system dynamics by a single first-order equation unlike the resonant energy harvesting problem [3,15,17].

2.2. Electromechanical frequency response

If the dynamic pressure uniformly acting on the stack shown in Fig. 1 is harmonic of the form $p(t) = p_0e^{j\omega t}$ (where p_0 is the amplitude of the axial pressure, ω is the frequency, and j is the unit imaginary number), then the steady-state voltage response

[1] In other words, the stack is excited at its off-resonant, quasi-static frequencies. This is a realistic assumption for energy harvesting at frequencies below kHz regime using a stack of fundamental resonance frequency on the order of tens of kHz.

can be expressed as $v(t) = Ve^{j\omega t}$, where the complex voltage V can be derived from Eq. (3) as

$$V = \frac{j\omega A d_{33}^{eff} p_0}{j\omega C_p^{eq} + (1/R_l)}. \tag{4}$$

The voltage output-to-pressure input frequency response function (FRF) can then be defined at steady state as

$$\alpha(\omega) = \frac{Ve^{j\omega t}}{p_0 e^{j\omega t}} = \frac{j\omega A d_{33}^{eff}}{j\omega C_p^{eq} + (1/R_l)}, \tag{5}$$

which can be used for steady-state power calculation at a given excitation frequency.

2.3. Power output and optimal electrical load

The electrical power (P) harvested from the stack under harmonic loading can be expressed as[2]

$$P = \frac{|V|^2}{R_l} = \frac{(\omega A d_{33}^{eff} p_0)^2 R_l}{(\omega C_p^{eq} R_l)^2 + 1}, \tag{6}$$

and therefore the optimal electrical load (R_l^*) that gives the maximum power output is

$$\left.\frac{\partial P}{\partial R_l}\right|_{R_l = R_l^*} = 0 \rightarrow R_l^* = \frac{1}{\omega C_p^{eq}}. \tag{7}$$

Back substitution of Eq. (7) into Eq. (6) leads to the following expression for maximum power output at the excitation frequency ω:

$$P_{\max} = P\big|_{R_l = R_l^*} = \frac{\omega (A d_{33}^{eff} p_0)^2}{2 C_p^{eq}}. \tag{8}$$

It is worth noting that $P_{\max} \propto (d_{33}^{eff})^2 / C_p^{eq}$ provides a metric to choose the optimal material for energy harvesting from low-frequency excitation of piezoelectric stacks. In view of the relations $d_{33}^{eff} = N\mu d_{33}$ and $C_p^{eq} = N\lambda \varepsilon_{33}^T A/h$, for stacks made of the same number of piezoelectric layers and under identical fabrication conditions, $d_{33}^2/\varepsilon_{33}^T$ is a reasonable FOM (figure of merit) for performance comparison (assuming similar change of the material properties with respect to their individual bulk properties when fabricated and assembled to form a stack). Table 1 shows a comparison of this FOM for various piezoelectric ceramics and single crystals. The properties of PMN-PT (with 33% PT) are due to Cao et al. [54] while the properties of PMN-PZT and PMN-PZT-Mn are from Zhang et al. [55], and the properties of the ceramics PZT-5A, PZT-5H, and PZT-8 are from the standard literature of piezoelectric ceramics [56]. Soft piezoelectric ceramics (e.g. PZT-5H and PZT-5A) offer larger power as compared to hard ceramics (e.g. PZT-8), and likewise, soft single crystals (e.g. PMN-PT and PMN-PZT) offer larger power as compared to hard single crystals (e.g. PMN-PZT-Mn); and furthermore, single crystals (e.g. PMN-PT and PMN-PZT) generate more power than standard ceramics (e.g. PZT-5H and PZT-5A) for low-frequency, off-resonant excitation in 33-mode, as summarized in Fig. 2. Therefore, unlike resonant energy harvesting, the quality factor has no effect, and hard ceramics/single crystals should be avoided in the present problem.

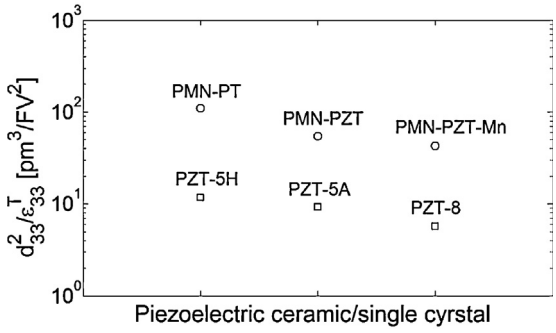

Fig. 2. Comparison of the FOM in low-frequency off-resonant power generation from piezoelectric ceramics (PZT-5A, PZT-5H, PZT-8) and single-crystals (PMN-PT, PMN-PZT).

2.4. Periodic excitation and steady-state response

If the pressure input is periodic of the form

$$p(t) = p(t+T), \tag{9}$$

where T is the period, then its Fourier series expansion is

$$p(t) = a_0 + \sum_{k=1}^{\infty} \left[a_k \cos\left(k\frac{2\pi t}{T}\right) + b_k \sin\left(k\frac{2\pi t}{T}\right) \right], \tag{10}$$

where a_0 is the mean value, while a_k and b_k ($k = 1, 2, \ldots$ are positive integers) are the Fourier coefficients given by

$$a_0 = \frac{1}{T}\int_0^T p(t)dt, \quad a_k = \frac{2}{T}\int_0^T p(t)\cos\left(k\frac{2\pi t}{T}\right)dt, \quad b_k = \frac{2}{T}\int_0^T p(t)\sin\left(k\frac{2\pi t}{T}\right)dt. \tag{11}$$

Since the steady-state voltage response to static pressure component is zero and the series has to be truncated after a finite number of terms (i.e. N terms), the steady-state periodic voltage output becomes

$$v(t) \cong \sum_{k=1}^{N} \left|\alpha\left(\frac{2\pi k}{T}\right)\right| \left\{ a_k \cos\left[\left(\frac{2\pi k t}{T}\right) + \phi\left(\frac{2\pi k}{T}\right)\right] + b_k \sin\left[\left(\frac{2\pi k t}{T}\right) + \phi\left(\frac{2\pi k}{T}\right)\right]\right\}, \tag{12}$$

where $\phi(\omega)$ is the phase of the voltage FRF $\alpha(\omega)$. The periodic power output can then be obtained from the following expression:

$$P(t) \cong \frac{1}{R_l}\left\langle \sum_{k=1}^{N} \left|\alpha\left(\frac{2\pi k}{T}\right)\right| \left\{ a_k \cos\left[\left(\frac{2\pi k t}{T}\right) + \phi\left(\frac{2\pi k}{T}\right)\right] + b_k \sin\left[\left(\frac{2\pi k t}{T}\right) + \phi\left(\frac{2\pi k}{T}\right)\right]\right\}\right\rangle^2. \tag{13}$$

It is useful to recall that the voltage FRF $\alpha(\omega)$ given by Eq. (5) is defined for the quasistatic frequencies of the stack, and therefore, the highest Fourier frequency $2N\pi/T$ required to represent the periodic pressure is assumed to be much less than the fundamental resonance frequency of the harvester stack, which is a realistic assumption for typical stochastic excitation mechanisms in conventional engineering systems.

[2] Note that the average power is simply half of the peak power: $P_{ave} = P/2$.

Table 1
Relevant piezoelectric and dielectric constants of various piezoelectric ceramics and single crystals and the figure of merit for off-resonant excitation in 33-mode (ε_0 = 8.854 pF/m).

	Soft and hard ceramics			Soft and hard single crystals		
	PZT-5H	PZT-5A	PZT-8	PMN-PT	PMN-PZT	PMN-PZT-Mn
d_{33} [pm/V]	593	374	225	2820	1530	1140
$\varepsilon_{33}^T/\varepsilon_0$	3400	1700	1000	8200	4850	3410
FOM = $d_{33}^2/\varepsilon_{33}^T$ [pm^3/FV^2]	11.7	9.3	5.7	109.5	54.5	43.0

3. Band-limited stochastic excitation and electromechanical response

3.1. Analytical approach: frequency-domain solution

First the frequency-domain analytical solution for mean power output is derived for off-resonant stochastic excitation of the stack. If band-limited random excitation is assumed with a constant power spectral density (PSD) over the frequency range $[-\bar{\omega}, \bar{\omega}]$, i.e. the physical frequency content of the one-sided PSD is over the range of $[0, \bar{\omega}]$, then the expected value of the power output (mean power) becomes

$$E[P] = \int_{-\bar{\omega}}^{\bar{\omega}} \frac{S_0}{R_l} \left|\alpha(\omega)\right|^2 d\omega, \tag{14}$$

where the input PSD of the axial pressure excitation is S_0 for the physical range of $[0, \bar{\omega}]$. It is assumed in the foregoing mean power equation that the random process is stationary. The analytical solution for the expected power output is then

$$E[P] = \frac{S_0}{R_l} \int_{-\bar{\omega}}^{\bar{\omega}} \left| \frac{j\omega A d_{33}^{eff}}{j\omega C_p^{eq} + (1/R_l)} \right|^2 d\omega$$
$$= \frac{2S_0}{R_l} \left(\frac{d_{33}^{eff} A}{C_p^{eq}} \right)^2 \left[\bar{\omega} - \frac{\tan^{-1}(\bar{\omega} C_p^{eq} R_l)}{C_p^{eq} R_l} \right]. \tag{15}$$

For this special case of frequency-independent (constant) excitation PSD (which is simply filtered, or band-limited, white noise), the optimal electrical load that gives the maximum power can be extracted using

$$\frac{\partial}{\partial R_l} E[P] \bigg|_{R_l = R_l^*} = 0 \rightarrow 2[(\bar{\omega} C_p^{eq} R_l^*)^2 + 1] \tan^{-1}(\bar{\omega} C_p^{eq} R_l^*)$$
$$- \bar{\omega} C_p^{eq} R_l^* [(\bar{\omega} C_p^{eq} R_l^*)^2 + 2] = 0. \tag{16}$$

Note that, the expected power for a given frequency-dependent PSD can be obtained from

$$E[P] = \frac{1}{R_l} \int_{-\bar{\omega}}^{\bar{\omega}} S(\omega) |\alpha(\omega)|^2 d\omega, \tag{17}$$

where $S(\omega)$ is the PSD of the axial pressure excitation and $\bar{\omega}$ is its upper frequency limit.

3.2. Numerical approach # 1: Fourier series-based Runge–Kutta solution

The first numerical solution approach treats the given time series of the excitation in a deterministic fashion through its Fourier series representation truncated after N terms following Eq. (10):

$$p(t) \cong a_0 + \sum_{k=1}^{N} \left[a_k \cos\left(k \frac{2\pi t}{T}\right) + b_k \sin\left(k \frac{2\pi t}{T}\right) \right], \tag{18}$$

where T is the length of the time history of the applied axial pressure and the other terms are as defined in Eq. (11). Therefore the stochastic forcing is represented in a deterministic form and can be fed into the ordinary differential equation of the system:

$$\dot{v} = \frac{1}{C_p^{eq}} \left(d_{33}^{eff} A \dot{p} - \frac{1}{R_l} v \right), \tag{19}$$

where v is the voltage output and $\dot{p}$ is the time derivative of the applied pressure. The computation can be carried out by using an ordinary differential equation (ODE) solver, such as the ode45 algorithm in MATLAB that uses an explicit Runge–Kutta formulation. The time history of voltage output is obtained from the electromechanical ODE given by Eq. (19). Then the expected value of power output can be computed by using

$$E[P] = \frac{1}{T} \int_0^T \frac{v^2(t)}{R_l} dt = \frac{{\sigma_v}^2}{R_l}, \tag{20}$$

where σ_v is the standard deviation of the voltage response across the electrical load.

3.3. Numerical approach # 2: Euler–Maruyama solution

An alternative approach that can be used for solving Eq. (3) in the case of random excitation is to treat the problem as a stochastic differential equation (SDE) and use the Euler–Maruyama method [57]. Using the Euler–Maruyama scheme, the voltage output is approximated by

$$dv = -\frac{v}{R_l C_p^{eq}} dt + \frac{d_{33}^{eff} A}{C_p^{eq}} dW, \tag{21}$$

where v is the voltage response and dW is the increment of the Wiener process (pressure input). In this case dW is simply the increment of dynamic pressure exerted on the stack dp, that is,

$$dW = dp. \tag{22}$$

For a given electrical load resistance, after obtaining the time history of voltage output using the Euler–Maruyama scheme, the mean power output can be computed using Eq. (20).

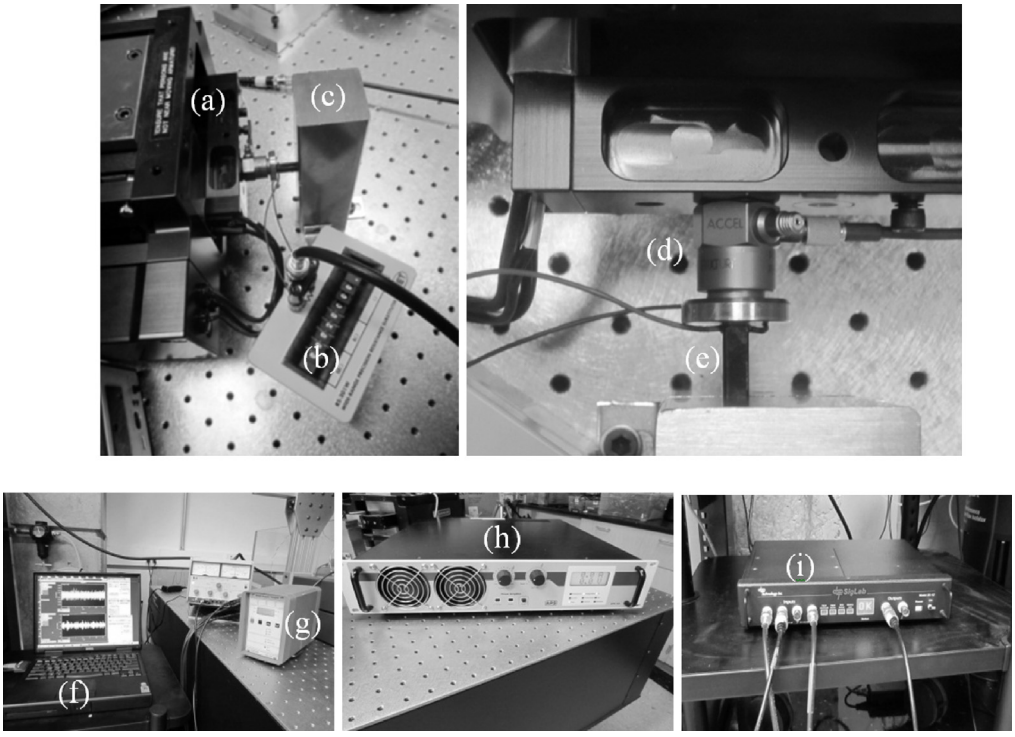

Fig. 3. Experimental setup: (a) electromagnetic shaker; (b) resistor box; (c) stiff fixture; (d) force transducer; (e) piezoelectric stack; (f) computer with data acquisition software; (g) signal conditioner; (h) amplifier; and (i) data acquisition hardware.

4. Results and experimental validation

4.1. Experimental setup and piezoelectric stack

A PZT-5H piezoelectric multilayer stack (TS18-H5-104 by Piezo Systems Inc.) is used in the experiments. The overall geometric, electromechanical, and dielectric properties of the stack are listed in Table 2. In the experimental setup (Fig. 3), the stack is horizontally compressed by a long-stroke shaker that is capable of creating excitation at low frequencies. A force transducer is located in series between the stack and the moving armature of the shaker. A resistor box is connected to the electrode terminals of the stack and voltage across the electrical load is measured for several resistance values in order to capture the optimal resistance for maximum power output. Two input channels of the data acquisition system are used; one records the force processed by a signal conditioner while the other records the voltage measured across the resistive load. The effective piezoelectric constant is identified from one single measurement under harmonic excitation as $d_{33}^{eff} = 110.5$ nm/V while the equivalent capacitance is measured to be $C_p^{eq} = 1745$ nF. The total number of piezoelectric layers in a broken sample is counted to be $N = 147$ from a micro-scale picture (Fig. 4). The fundamental resonance frequency of the PZT-5H piezoelectric stack used in the experiments is 74 kHz according to the manufacturer (Piezo Systems Inc.). Therefore, all practical excitation frequencies are within the off-resonant quasi-static region of the stack, in agreement with the theoretical modeling efforts given in this work based on first-order system dynamics.

Table 2
Geometric, piezoelectric, and dielectric properties of the PZT-5H stack.

Cross section [mm^2]	5×5
Height [mm]	18
d_{33}^{eff} [nm/V]	110.5
C_p^{eq} [nF]	1745

4.2. Electromechanical frequency response

Prior to harmonic and stochastic loading experiments, chirp tests are conducted for the purpose of obtaining the electromechanical response FRFs of the system for a range of electrical load resistance values. Chirp excitation is provided for the frequency range of 0–200 Hz and 5 averages are taken for each resistive load. Fig. 5 shows that the analytical voltage output FRFs are in excellent agreement with the experimental results for a set of resistors. The experimental FRF measurements focus on the low-frequency off-resonant range in agreement with the model FRF given by Eq. (5). Having validated the electromechanical frequency response of the system for a broad range of resistance values ranging from short- to open-circuit conditions, harmonic and stochastic excitation experiments are conducted next.

4.3. Harmonic excitation

In the harmonic excitation experiments, the stack is subjected to excitation at three different frequencies (10, 20, and 30 Hz) and resistor sweep tests are performed. At each frequency, the stack is compressed by harmonic force with five different voltage input

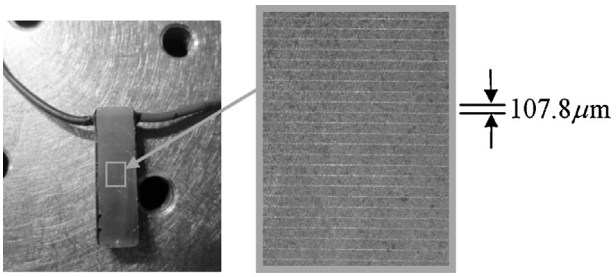

Fig. 4. Close-up picture of the piezoelectric stack and micro-scale picture detail of the layers after the external coat is removed.

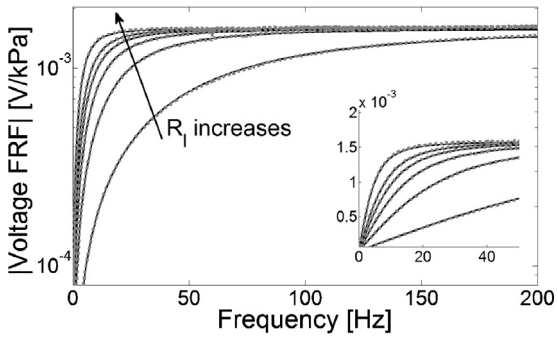

Fig. 5. Voltage output-to-pressure input FRFs of the PZT-5H stack for a set of resistors (R_l = 999, 2991, 4975, 6951, 8920, 14,778 Ω). Solid lines: analytical; dashed lines: experimental.

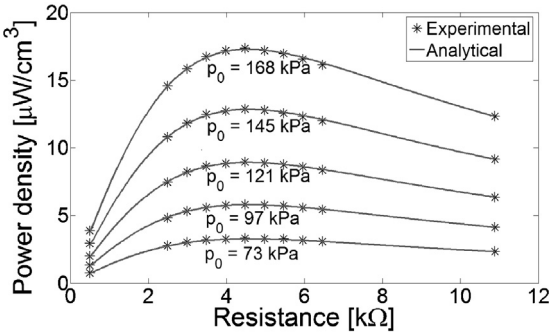

Fig. 6. Power output (normalized with respect to the stack volume) versus electrical load resistance under harmonic excitation at 20 Hz for different pressure levels.

levels to the shaker (Fig. 3a), resulting in five pressure levels exerted to the stack. The experimental measurements of harvested power are compared to analytical solutions computed using Eq. (6). For harmonic excitation at 20 Hz, the comparisons are shown in Fig. 6 as the power output per stack volume, i.e. power density of the harvester.

It is useful to further normalize the electrical power output with respect to excitation amplitude. We note from Eq. (6) that the power output is quadratically proportional to the square of the input pressure amplitude. The resulting power density normalized with respect to input pressure squared is shown in Fig. 7, which reduces the five curves of Fig. 5 into a single curve from which one can predict the maximum power output for different device volume and presume amplitudes at a fixed frequency (20 Hz in Fig. 7). This confirms the linear behavior of the system at these frequencies and excitation levels.

Finally, the maximum power behavior with changing excitation pressure at different frequencies can be explored using Eq.

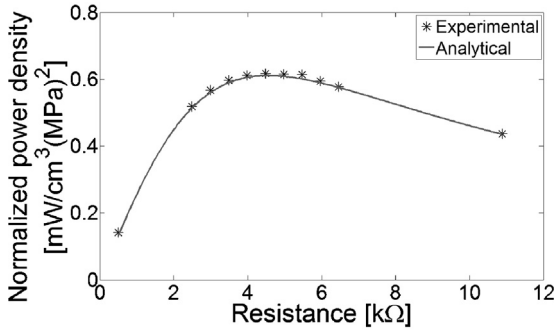

Fig. 7. Power output (normalized with respect to the stack volume and pressure input) versus electrical load resistance under harmonic excitation at 20 Hz.

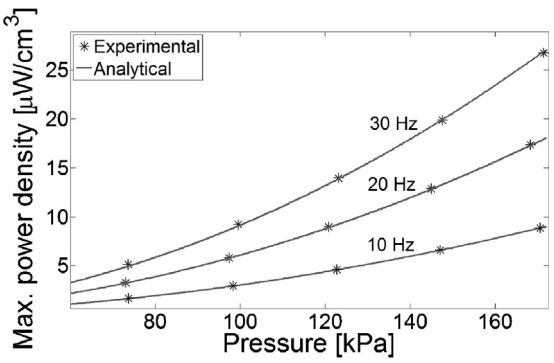

Fig. 8. Maximum power output (normalized with respect to the stack volume) under harmonic excitation at 10 Hz, 20 Hz and 30 Hz versus pressure amplitude.

(8). Quadratic dependence between the power output and excitation pressure is clearly observed in Fig. 8 at each excitation frequency. Overall the analytical solution and experimental measurements exhibit excellent agreement, validating the sufficiency of a single first-order equation to represent the system dynamics for low-frequency off-resonant energy harvesting from axial pressure excitation of a piezoelectric stack.

4.4. Band-limited stochastic excitation

Stochastic excitation of the stack is explored next by applying band-limited random input. A sample of time history of the applied axial pressure in one test is shown in Fig. 9 along with its PSD. As can be observed from the PSD, the input energy provided to the shaker is concentrated within the 0–200 Hz band. This is a frequency range that covers the effective PSD range of typical ambient kinetic and vibration energy sources [11]. One should note that the experimental PSD in Fig. 9 is not an ideal band-limited (filtered) white noise. Therefore, Eq. (17) must be used instead of Eq. (15) in order to predict the expected value of the power output.

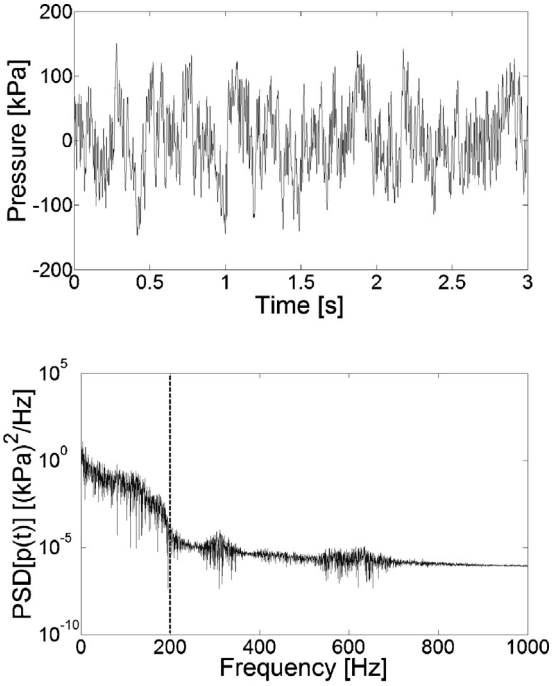

Fig. 9. An experimental time history example for band-limited stochastic pressure excitation applied to the stack (RMS pressure: 58 kPa) and its PSD.

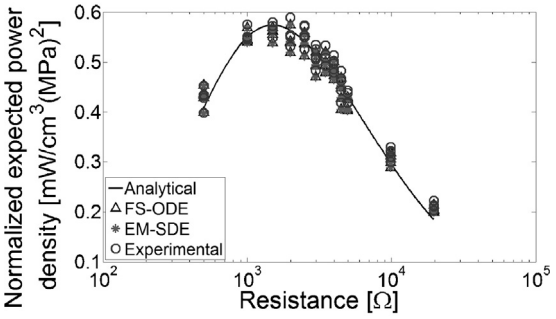

Fig. 10. Comparison of experimental results, numerical simulations, and analytical predictions of power generation (normalized with respect to the stack volume and pressure input) versus load resistance at an RMS pressure level 58 kPa (FS-ODE: Fourier series-based ODE solution, EM-SDE: Euler–Maruyama scheme for SDE solution).

When performing integration in the analytical solution by using the experimentally obtained PSD of the pressure input ($S(\omega)$ in Eq. (17)), the upper frequency limit is taken as 200 Hz based on Fig. 9. Resistor sweep experiments are then conducted from 500 Ω to 20 kΩ (12 resistors are used) for an RMS (root-mean-square) pressure input level of 58 kPa. In each set of experiments, signals of force input and voltage output are recorded for 3.2 s. The experimental measurements are plotted and compared against the analytical and numerical predictions in Fig. 10. For each resistive load, the test is repeated 5 times to ensure the repeatability of the statistical measures of the input and output (yielding a total of 60 measurements for 12 different resistors). From Eq. (17), the expected (mean) power is computed in the frequency-domain solution by using the experimental PSD of one case, while the individual time histories of excitation (60 different time series) are used in the ODE-based and SDE-based numerical simulations for each resistor. Once the voltage histories are obtained for a given resistor in the numerical solutions, Eq. (20) is used to calculate the expected power. Overall, very good agreement is observed between the experimental results and model predictions by both analytical and numerical solutions.

As the last graph of practical interest, the maximum expected power versus RMS pressure is plotted in Fig. 11. A quadratic relation between maximum power and pressure is observed for band-limited stochastic excitation as well. This is due to the quadratic relation between pressure and its PSD (while the power output is linearly proportional to the PSD of pressure). According to Figs. 10 and 11, micro-watt to milli-watt level stochastic power can be extracted as the pressure input is changed from kPa to MPa level.

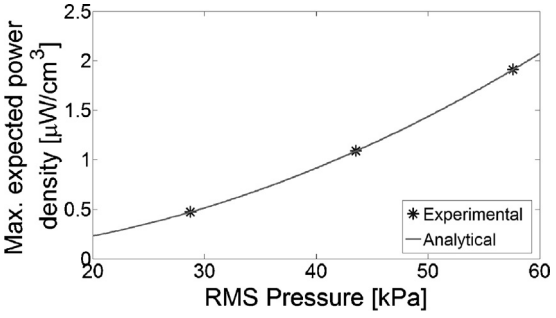

Fig. 11. Experimental results and analytical predictions of maximum expected power output at different RMS pressure levels.

5. Conclusions

In this paper, deterministic and band-limited stochastic energy harvesting scenarios using a multilayer piezoelectric stack under uniaxial dynamic pressure loading are explored theoretically and experimentally. The motivation for this off-resonant energy harvesting problem derives from typical civil infrastructure systems subjected to dynamic compressive forces in deterministic or band-limited stochastic forms due to vehicular or human loads, among other examples of compressive loading in low-frequency region of piezoelectric stacks. Frequency-domain analytical solutions for harmonic, periodic, and band-limited stochastic uniaxial loading are presented for this first-order problem. In addition, time-domain numerical solutions for power generation under band-limited stochastic excitation are presented. The first one of the two numerical solution methods uses the Fourier series representation of the excitation history to solve the resulting ordinary differential equation, while the second method employs an Euler–Maruyama scheme to directly solve the governing electromechanical stochastic differential equation. The analytical and numerical predictions exhibit very good agreement with the experimental measurements taken for a PZT-5H multilayer stack. The results are further validated for different levels of excitation intensity. The electromechanical model and solutions presented in this paper are shown to be reliable tools for predicting and optimizing the performance of piezoelectric stack harvesters under band-limited stochastic excitation due to dynamic compressive loads in various problems. The model given here is also used to extract the figure of merit for choosing the active material. It is concluded that soft piezoelectric ceramics (e.g. PZT-5H and PZT-5A) offer larger power as compared to hard ceramics (e.g. PZT-8), and likewise, soft single crystals (e.g. PMN-PT and PMN-PZT) offer larger power as compared to hard single crystals (e.g. PMN-PZT- Mn); and furthermore, single crystals (e.g. PMN-PT and PMN-PZT) generate more power than standard ceramics (e.g. PZT-5H and PZT-5A) for low-frequency, off-resonant excitation of piezoelectric stacks.

Acknowledgements

This project was supported by the U.S. Department of Commerce, National Institute of Standards and Technology, Cooperative Agreement Number 70NANB9H9007, “Self-Powered Wireless Sensor Network for Structural Health Prognosis.”

References

[1] S. Roundy, P.K. Wright, J.M. Rabaey, Energy Scavenging for Wireless Sensor Networks: With Special Focus on Vibrations, Springer, 2004.
[2] N.S. Hudak, G.G. Amatucci, Small-scale energy harvesting through thermoelectric, vibration, and radiofrequency power conversion, J. Appl. Phys. 103 (10) (2008), pp. 101301–101301-24.
[3] A. Erturk, D.J. Inman, Piezoelectric Energy Harvesting, Wiley, 2011.
[4] N. Elvin, A. Erturk, Advances in Energy Harvesting Methods, Springer, 2013.
[5] P. Glynne-Jones, et al., An electromagnetic, vibration-powered generator for intelligent sensor systems, Sens. Actuat. A-Phys. 110 (1–3) (2004) 344–349.
[6] D.P. Arnold, Review of microscale magnetic power generation, IEEE Trans. Magn. 43 (11) (2007) 3940–3951.
[7] N.G. Elvin, A.A. Elvin, An experimentally validated electromagnetic energy harvester, J. Sound Vibr. 330 (10) (2011) 2314–2324.
[8] A. Rahimi, et al., An electromagnetic energy harvesting system for low frequency applications with a passive interface ASIC in standard CMOS, Sens. Actuat. A: Phys. 188 (2012) 158–166.
[9] N.A. Aboulfotoh, M.H. Arafa, S.M. Megahed, A self-tuning resonator for vibration energy harvesting, Sens. Actuat. A: Phys. 201 (2013) 328–334.
[10] H. Liu, Y. Qian, C. Lee, A multi-frequency vibration-based MEMS electromagnetic energy harvesting device, Sens. Actuat. A: Phys. 204 (2013) 37–43.
[11] S. Roundy, P.K. Wright, J. Rabaey, A study of low level vibrations as a power source for wireless sensor nodes, Comput. Commun. 26 (11) (2003) 1131–1144.
[12] P.D. Mitcheson, et al., MEMS electrostatic micropower generator for low frequency operation, Sens. Actuat. A-Phys. 115 (2–3) (2004) 523–529.
[13] C.P. Le, et al., Microscale electrostatic energy harvester using internal impacts, J. Intell. Mater. Syst. Struct. 23 (13) (2012) 1409–1421.

[14] S. Roundy, P.K. Wright, A piezoelectric vibration based generator for wireless electronics, Smart Mater. Struct. 13 (5) (2004) 1131–1142.
[15] N.E. DuToit, B.L. Wardle, Experimental verification of models for microfabricated piezoelectric vibration energy harvesters, AIAA J. 45 (5) (2007) 1126–1137.
[16] Y. Shu, I. Lien, Analysis of power output for piezoelectric energy harvesting systems, Smart Mater. Struct. 15 (6) (2006) 1499.
[17] A. Erturk, D.J. Inman, An experimentally validated bimorph cantilever model for piezoelectric energy harvesting from base excitations, Smart Mater. Struct. 18. (2) (2009).
[18] R. Ly, et al., Modeling and characterization of piezoelectric cantilever bending sensor for energy harvesting, Sens. Actuat. A: Phys. 168 (1) (2011) 95–100.
[19] L. Zhou, et al., A model for the energy harvesting performance of shear mode piezoelectric cantilever, Sens. Actuat. A: Phys. 179 (2012) 185–192.
[20] J.et al. Nunes-Pereira, Energy harvesting performance of piezoelectric electrospun polymer fibers and polymer/ceramic composites, Sens. Actuat. A: Phys. 196 (2013).
[21] L. Wang, F.G. Yuan, Vibration energy harvesting by magnetostrictive material, Smart Mater. Struct. 17 (4) (2008).
[22] A. Adly, et al., Experimental tests of a magnetostrictive energy harvesting device toward its modeling, J. Appl. Phys. 107 (9) (2010).
[23] P.-J. Cottinet, D. Guyomar, M. Lallart, Electrostrictive polymer harvesting using a nonlinear approach, Sens. Actuat. A: Phys. 172 (2) (2011) 497–503.
[24] F. Belhora, et al., Hybridization of electrostrictive polymers and electrets for mechanical energy harvesting, Sens. Actuat. A: Phys. 183 (2012) 50–56.
[25] R.D. Kornbluh, et al., From boots to buoys: promises and challenges of dielectric elastomer energy harvesting, in: SPIE Smart Structures and Materials + Nondestructive Evaluation and Health Monitoring, International Society for Optics and Photonics, 2011.
[26] M. Aureli, et al., Energy harvesting from base excitation of ionic polymer metal composites in fluid environments, Smart Mater. Struct. 19 (1) (2010) 015003.
[27] H. Liu, et al., Piezoelectric MEMS-based wideband energy harvesting systems using a frequency-up-conversion cantilever stopper, Sens. Actuat. A: Phys. 186 (2012) 242–248.
[28] M. Renaud, et al., Fabrication, modelling and characterization of MEMS piezoelectric vibration harvesters, Sens. Actuat. A: Phys. 145 (2008) 380–386.
[29] Y. Jeon, et al., MEMS power generator with transverse mode thin film PZT, Sens. Actuat. A: Phys. 122 (1) (2005) 16–22.
[30] R. Xu, et al., Screen printed PZT/PZT thick film bimorph MEMS cantilever device for vibration energy harvesting, Sens. Actuat. A: Phys. 188 (2012) 383–388.
[31] H.A. Sodano, D.J. Inman, G. Park, A review of power harvesting from vibration using piezoelectric materials, Shock Vibr. Dig. 36 (3) (2004) 197–206.
[32] S.R. Anton, H.A. Sodano, A review of power harvesting using piezoelectric materials (2003–2006), Smart Mater. Struct. 16 (3) (2007) R1.
[33] S. Priya, Advances in energy harvesting using low profile piezoelectric transducers, J. Electroceram. 19 (1) (2007) 167–184.
[34] K.A. Cook-Chennault, N. Thambi, A.M. Sastry, Powering MEMS portable devices—a review of non-regenerative and regenerative power supply systems with special emphasis on piezoelectric energy harvesting systems, Smart Mater. Struct. 17 (4) (2008) 043001.
[35] S. Sherrit, et al., Multilayer piezoelectric stack actuator characterization, in: The 15th International Symposium on: Smart Structures and Materials & Nondestructive Evaluation and Health Monitoring, International Society for Optics and Photonics, 2008.
[36] X. Jing, J. Su, T.-B. Xu, Piezoelectric Multilayer-stacked Hybrid Actuation/Transduction System. 2009, Google Patents.
[37] T.-B. Xu, et al., Energy harvesting using a PZT ceramic multilayer stack, Smart Mater. Struct. 22 (6) (2013) 065015.
[38] M. Goldfarb, L. Jones, On the efficiency of electric power generation with piezoelectric ceramic, Trans. ASME J. Dyn. Syst. Meas. Contr. 121 (1999) 566–571.
[39] J. Feenstra, J. Granstrom, H. Sodano, Energy harvesting through a backpack employing a mechanically amplified piezoelectric stack, Mech. Syst. Signal Process. 22 (3) (2008) 721–734.
[40] H.W. Kim, et al., Energy harvesting using a piezoelectric "Cymbal" transducer in dynamic environment, Jpn. J. Appl. Phys. 43 (2004) 6178.
[41] X. Li, M. Guo, S. Dong, A flex-compressive-mode piezoelectric transducer for mechanical vibration/strain energy harvesting, IEEE Trans. Ultrason. Ferroelectr. Freq. Contr. 58 (4) (2011) 698–703.
[42] E. Halvorsen, Energy harvesters driven by broadband random vibrations, J. Microelectromech. Syst. 17 (5) (2008) 1061–1071.
[43] S. Adhikari, M. Friswell, D. Inman, Piezoelectric energy harvesting from broadband random vibrations, Smart Mater. Struct. 18 (11) (2009) 115005.
[44] S. Zhao, A. Erturk, Electroelastic modeling and experimental validations of piezoelectric energy harvesting from broadband random vibrations of cantilevered bimorphs, Smart Mater. Struct. 22 (1) (2013) 015002.
[45] M.F. Daqaq, Response of uni-modal duffing-type harvesters to random forced excitations, J. Sound Vibr. 329 (18) (2010) 3621–3631.
[46] D.A. Barton, S.G. Burrow, L.R. Clare, Energy harvesting from vibrations with a nonlinear oscillator, Trans. ASME-L-J. Vibr. Acoust. 132 (2) (2010) 021009.
[47] G. Litak, M. Friswell, S. Adhikari, Magnetopiezoelastic energy harvesting driven by random excitations, Appl. Phys. Lett. 96 (21) (2010), pp. 214103–214103-3.
[48] M.F. Daqaq, Transduction of a bistable inductive generator driven by white and exponentially correlated Gaussian noise, J. Sound Vibr. 330 (11) (2011) 2554–2564.
[49] L. Gammaitoni, I. Neri, H. Vocca, Nonlinear oscillators for vibration energy harvesting, Appl. Phys. Lett. 94 (16) (2009).
[50] F. Cottone, H. Vocca, L. Gammaitoni, Nonlinear energy harvesting, Phys. Rev. Lett. 102 (8) (2009) 080601.
[51] S. Zhao, A. Erturk, On the stochastic excitation of monostable and bistable electroelastic power generators: Relative advantages and tradeoffs in a physical system, Appl. Phys. Lett. 102 (10) (2013), pp. 103902–103902-5.
[52] P. Kumar, et al., Fokker–Planck equation analysis of randomly excited nonlinear energy harvester, J. Sound Vibr. 333 (7) (2014) 2040–2053.
[53] W. Martens, U. von Wagner, G. Litak, Stationary response of nonlinear magnetopiezoelectric energy harvester systems under stochastic excitation, Eur. Phys. J. Spec. Top. 222 (7) (2013) 1665–1673.
[54] H. Cao, et al., Elastic, piezoelectric, and dielectric properties of $^{0.58}$Pb (MgNb) O–$^{0.42}$PbTiO single crystal, J. Appl. Phys. 96 (2004) 549.
[55] S. Zhang, et al., Characterization of mn-modified Pb ($Mg_{1/3}$ $Nb_{2/3}$) O_3–$PbZrO_3$–$PbTiO_3$ single crystals for high power broad bandwidth transducers, Appl. Phys. Lett. 93 (12) (2008), pp. 122908–122908-3.
[56] www.efunda.com/materials/piezo/material_data
[57] P.E. Kloeden, R. Pearson, The numerical solution of stochastic differential equations, J. Aust. Math. Soc. Ser. B. Appl. Math. 20 (01) (1977) 8–12.

Biographies

S. Zhao received her M.S. (2013) in Mechanical Engineering from Georgia Institute of Technology and B.S. (2011) in Mechanical Engineering (with a minor in Mathematics) from Miami University. During her graduate studies at Georgia Tech, she received various awards including the 2013 "Best M.S. Thesis Award" of the Sigma Xi Georgia Tech Chapter for her thesis on "Energy Harvesting from Random Vibrations of Piezoelectric Cantilevers and Stacks" and the "Best Student Paper Award" of the 2012 ASME Conference on Smart Materials, Adaptive Structures and Intelligent Systems (SMASIS).

A. Erturk is an Assistant Professor of Mechanical Engineering at Georgia Institute of Technology. His current theoretical and experimental research interests are centered on the intersection of electroelastic structures and dynamical systems for novel multi-physics problems such as vibration-based energy harvesting and bio-inspired locomotion. He has published more than 100 articles in journals and conference proceedings, authored a book titled Piezoelectric Energy Harvesting (Wiley, 2011), and co-edited a book titled Advances in Energy Harvesting Methods (Springer, 2013). He is an Elected Member of the ASME Adaptive Structures and Material Systems Branch (2011-) and the ASME Technical Committee on Vibration and Sound (2011-2017), the Founding Chair of the ASME Energy Harvesting Technical Committee (2012-2014), an Associate Editor for the journal Smart Materials and Structures and for the Journal of Intelligent Material Systems and Structures. Dr. Erturk received his Ph.D. in Engineering Mechanics from Virginia Tech in 2009; M.S. and B.S. in Mechanical Engineering from METU (Ankara, Turkey), in 2006 and 2004, respectively. He has received various awards including an NSF CAREER Award (2013) in Dynamical Systems.